

# Experimental Investigation on Synthesis and Characterization of Self-Cleaning Modified Super Hydrophobic Nano-SiO<sub>2</sub> Coating for Solar Photovoltaic Applications: Effects of HDTMS and TEA

Abhineet Samadhiya<sup>a,b</sup>, Pradeep Kumar Jhinge<sup>b</sup>, Kamal Kumar Kushwah<sup>c\*</sup>

<sup>a</sup>Rajiv Gandhi Proudhyogiki Vishwavidyalaya, Bhopal 462 033, India

<sup>b</sup>Department of Mechanical Engineering, Jabalpur Engineering College, Jabalpur 482 011, India

<sup>c</sup>Department of Applied Physics, Jabalpur Engineering College, Jabalpur 482 011, India

*Received: 8 April 2023; Accepted: 13 June 2023*

Solar photovoltaics is a significant renewable energy source. However, solar PV panels' efficiency decreases due to dust accumulation on their surface, leading to decreased power and increased maintenance costs. A super-hydrophobic, optically transparent, and self-cleaning modified nano-coatings have been synthesized using HDTMS-nano-silica and applied as a top-glass cover on solar PV cells to address this issue. The nano-coating is found to improve the efficiency of the PV panels and reduce the cleaning costs.

In the first phase, modified HDTMS-nano-SiO<sub>2</sub> coatings are synthesized using HDTMS and triethyl amine. The x-ray diffraction (XRD) and energy dispersive x-ray (EDX) studies have confirmed the presence of silica nanoparticles and successful modification to HDTMS-nano-SiO<sub>2</sub>. Five potential samples have been characterized using scanning electron microscopy (SEM), and the hydrophobicity is tested using a water contact angle test (WCA). Thermogravimetric analysis (TGA) studies have revealed the stability of HDTMS-nano-SiO<sub>2</sub> at higher temperatures, and demonstrational assessment of transparency is also tested.

In the second phase, the environmental stability of the HDTMS-nano-SiO<sub>2</sub> coating is evaluated using three identical solar PV cells. The experimental results demonstrated that nanomaterial-coated-uncleaned solar PV cells outperform uncoated-dusty-uncleaned solar PV cells efficiency by 16% and regularly physically cleaned uncoated solar PV cells efficiency by 6.5%. The nano-coating has a 35-day active duration.

The synthesized HDTMS-nano-SiO<sub>2</sub> coating proves to be a cost-effective solution to improve solar PV panels' efficiency by reducing dust accumulation and minimizing cleaning costs. The study demonstrates the potential of self-cleaning nano-coatings for enhancing the performance of solar PV panels.

**Keywords:** Superhydrophobic transparent coating, Photovoltaics, Hexadecyltrimethoxysilane (HDTMS), Optically transparent nanocoating, Triethylamine (TEA)

## 1 Introduction

Nano-SiO<sub>2</sub> has a huge specific surface area and is odorless, non-toxic, and lightweight<sup>1</sup>. It has good mechanical, optical, mechanical, and flame-retardant qualities. It has drawn a lot of interest in the industries of ceramics, papermaking, metals, plastics, photovoltaics, and many more<sup>2-7</sup>. Due to their wide range of uses, including dirt resistance, corrosion resistance, anti-icing characteristics, and others, surfaces with hydrophobic properties have sparked a lot of curiosity<sup>8</sup>. Superhydrophobic surfaces have been produced by manipulating both chemical composition and morphological structure, and they are now widely acknowledged to be the outcome of

the interaction between high surface roughness and low surface energy<sup>9</sup>. A diverse and wide range of bottom-up and top-down research teams have attempted to create fabrication methods for superhydrophobic surfaces<sup>10</sup>. Clear superhydrophobic coatings are gaining popularity lately in the context of transparent optical purposes like solar cells, windows, and lenses<sup>10</sup>. However, creating such surfaces has frequently required time-consuming or expensive procedures, and necessitated ineffective methods because of lack of wear resistance or needed surface pre- or post-treatment for a wide range of substrates and particles<sup>11</sup>.

The impact of surface morphology on transparency and hydrophobicity has been investigated, and more recently, a method for coating hydrophobic nano-

\* Corresponding author (E-mail: kamal\_kushwah2005@yahoo.com)

particles with silane to give them transparent superhydrophobic properties has been illustrated<sup>12</sup>. In this work, silica nanoparticles are used to demonstrate a straightforward technique for creating superhydrophobic transparent coatings. The adherent force amidst surfaced materials and the substrate can be increased using this technology without the need for extra surface treatments. By adjusting the solution's concentration of silica nanoparticles, the surface shape may be readily modified, which can be further managed to impart considerable superhydrophobic and transparent coatings.

## 2 Materials and Methods

### 2.1 Materials

Finely powdered silicon dioxide nanoparticles with average particle size (30-50 nm) were used for the research along with coupling agent silane, specifically hexadecyltrimethoxysilane(HDTMS). Without additional purification, the other reagents like triethylamine (TEA), distilled water, and ethanol absolute were utilized in their original form without any prior or after modifications. All chemicals were of analytical grade. The existence of SiO<sub>2</sub> at about 23°-25° has been confirmed by XRD of SiO<sub>2</sub> nanoparticles (Fig. 1)

### 2.2 Synthesis of the modified silica nano-particles

A chemical route was used for the synthesis of hybrid silica-nano particles with different SiO<sub>2</sub> concentrations. A 3.6-weight-percentage modified silica dispersion solution was made by dissolving 0.3 g nano-silica particles in 7.2 ml anhydrous ethanol and then 0.15 ml of HDTMS liquid solution was added to the resulting solution under ultrasonication

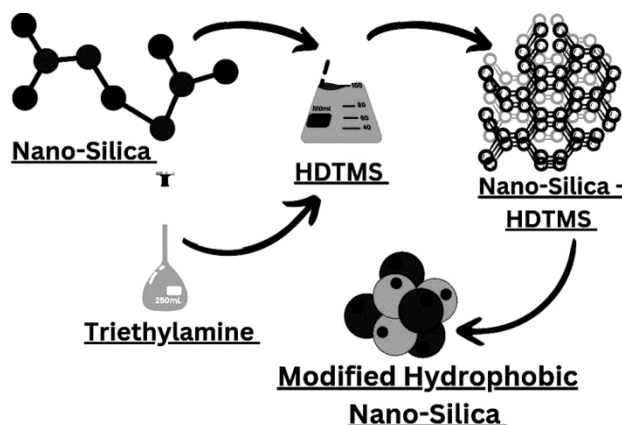


Fig. 1— Schematic diagram showing the preparation of Modified Hydrophobic Nano-SiO<sub>2</sub> coating.

for 15 minutes. Thus, transparent super hydrophobic modified Nano-SiO<sub>2</sub> layers were obtained. The PH of the solution was controlled by mixing triethylamine during ultrasonication and the resulting mixtures were left for 24 hours at room temperature conditions. Using the same method of experimentation, four other modified silica dispersion solutions were prepared with 0.3%, 0.6%, 2%, and 3.6-4% concentrations.

The chemistry involved in the mechanism of the formation of hydrophobically modified nano-silica layers should also be understood which gives a deep informational insight into the overall preparation process. The schematic diagram (Fig. 2) illustrates this chemistry mechanism involved in the formation of modified hydrophobic nano-silica layers.

It explains the role of triethylamine as a base that abstracts H<sup>+</sup> ions from the hydroxyl group of silicate moiety and leaves it as a stronger nucleophilic group that can attack the HDTMS. Further, stronger nucleophilic clusters on the silica surface favor better attachment of HDTMS with an oxygen atom and the removal of —OCH<sub>3</sub> groups into the medium. The —OCH<sub>3</sub> groups later abstract the H<sup>+</sup> ion back from the triethylammonium ion to regenerate the catalyst. A sincere attempt has been made to explain the above-mentioned mechanism through a schematic diagram representing the step-by-step process

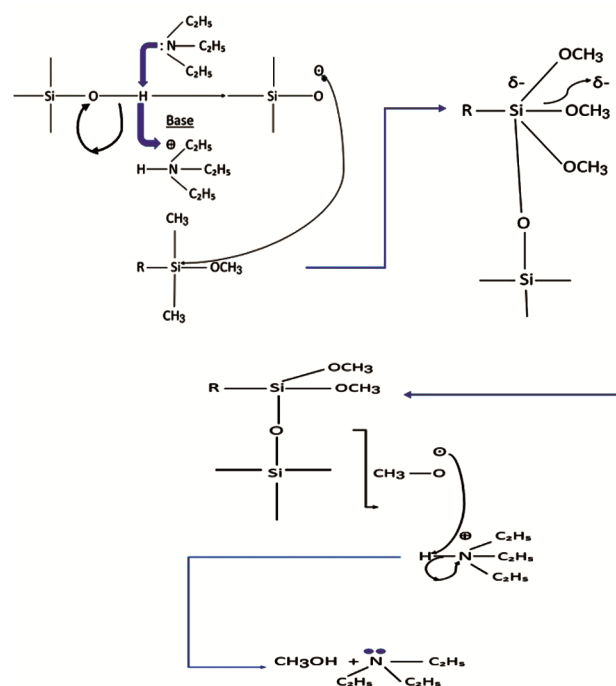


Fig. 2 — Schematic diagram showing the chemistry mechanism involved in the preparation of Modified Hydrophobic Nano-SiO<sub>2</sub> coating.

involved in forming hydrophobically modified silica nanolayers using different chemicals.

### 2.3 Silica nanoparticles dip-coating on a glass substrate preparation

Without any prior or after treatment, two pairs of 25mm x 75 mm glass slides were vertically lifted out of the dispersion solution above mentioned after 2 minutes and were allowed to dry at room temperature overnight in the preparation laboratory.

The EDX results shown in Figures 4a and 4b show successful grafting of silica nanoparticles on the above-discussed glass slides with the mentioned dimensions.

### 2.4 Characterization

A high-resolution SEM (scanning electron microscopy) (SEM, ZEISS, 10 kV), XRD (X-ray diffraction), and EDX (energy dispersive X-ray spectroscopy) were used to depict and analyze the morphologies of the material of all the samples. The CA100A device was used to measure the water contact angles, and a regulated 5  $\mu$ L droplet size of deionized water was used. TGA (thermo gravimetric analysis) study of original silica nanoparticles and modified HDTMS-nano silica nanoparticles was also performed to check the thermal stability of the prepared nano-coating at high temperatures.

## 3 Results and Discussions

### 3.1 XRD Analysis

Figure 3 represents the X-ray diffraction (XRD) pattern of silica nanoparticles. The typical peaks of the synthesized silica nanoparticle at the  $2\theta$  degree region ranged from  $23^\circ$  to  $25^\circ$ , which were discovered to be consistent with the standards.

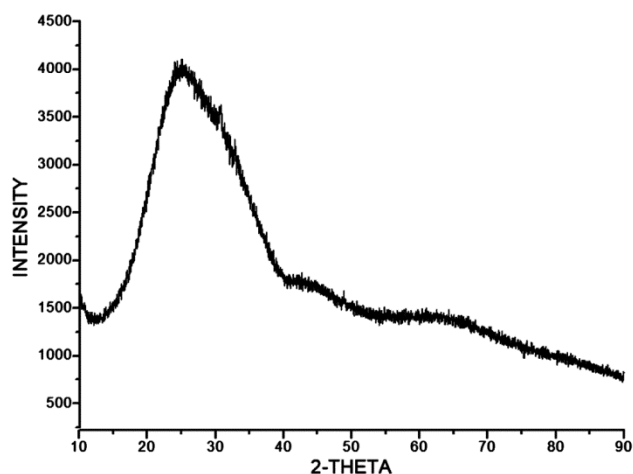


Fig. 3 — shows XRD spectra of SiO<sub>2</sub> nanoparticle.

The significantly wider diffraction peaks indicate that the synthesized powder particles were nanosized. Further, in Fig. 3, the XRD pattern has prominent diffraction peaks, and Bragg's reflections are visible. The purity of the silica nanoparticles is represented by the peaks.

These Bragg's reflections clearly showed the presence of sets of lattice planes. Further, on these grounds, they may be classified as face-centered cubic structures (fcc)<sup>13</sup> of silica nanoparticles created in our current synthesis, demonstrating that they are crystalline in nature.

### 3.2 EDX Analysis

In addition, the composition of the chemical elements of nano-SiO<sub>2</sub> and HDTMS-nano-SiO<sub>2</sub> was measured by energy dispersive x-ray analysis, shown by Figures 4 a, b.

The nano-SiO<sub>2</sub> elemental composition was solely O (Oxygen) and Si (Silicon), as shown by the comparative examination of the data in Figure 4a. Table 1 shows the respective weight percentages and atomic percentages of oxygen and silicon, representing the original silica nanoparticles to be modified.

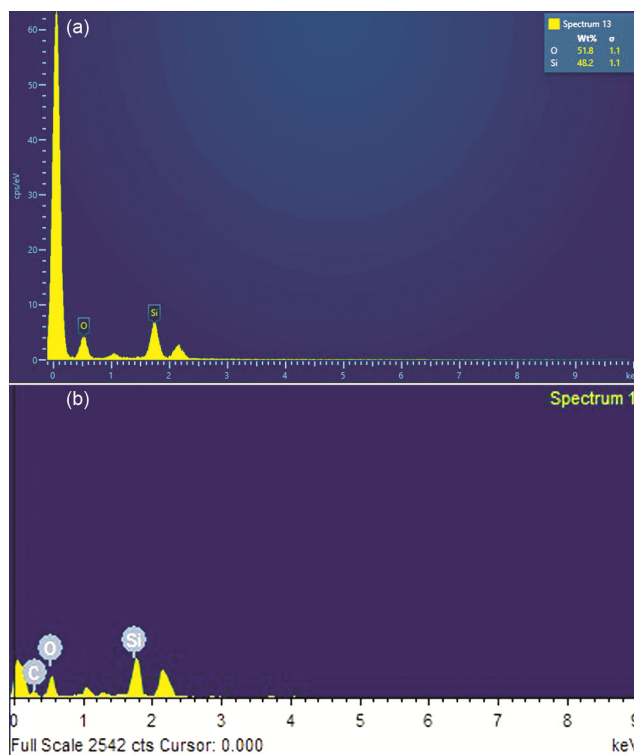


Fig. 4 — (a) EDX of original Silica Nanoparticles used for experimentation, & (b) EDX Result of the Silica Nanoparticles grafting on glass slides for experimentation.

After being altered, a specific amount of the element C was added to HDTMS-nano-SiO<sub>2</sub>, which proved that the material had been altered shown in Fig. 4b.

The C element first appeared as a result of the existence of CH<sub>2</sub> and CH<sub>3</sub>, resulting in providing hydrophobic behavior to material particles. Therefore, the study revealed the C element's presence in HDTMS-Nano silica<sup>14</sup>.

Table 2 shows the respective weight percentages and atomic percentages of carbon oxygen and silicon in which the presence of carbon weight and atomic percentages approves the modification of silica nanoparticles to HDTMS-nano-SiO<sub>2</sub> nanoparticles.

### 3.3 SEM Analysis

By diluting the silica nanoparticle concentration in anhydrous ethanol, the concentration of the solution was changed. In this work, a new form of silica

nanoparticles with a fusion of HDTMS and TEA was formed and an effort has been made to introduce information about the specific nature of the hydrophobicity property of nano-silica particles by mixing with HDTMS and TEA. The original glass slide surface's water contact angle was 52 degrees. The water contact angle increases as silica content rises, with the highest value occurring between concentrations of 0.5 and 1 weight percent<sup>1</sup>. The interaction of nano and micro hierarchical structures and low surface energy materials can be readily analyzed to explain WCA (water contact angle) analysis<sup>15</sup>. This finding also suggests that the optimum concentration of silica nanoparticles is crucial for producing superhydrophobic coatings. Surface roughness and low surface energy materials brought about by silane coupling agents (HDTMS) and silica nanoparticles are sources of a particular surface's hydrophobicity and superhydrophobicity.

With triethylamine acting as a hydrolysis catalyst at room temperature, HDTMS changes silane into silanol, which causes modified silica nanoparticles to stack up on the surface by interacting with the hydroxyl(-OH-) groups found on the surfaces of glass slides and silica nanoparticles.

Scanning electron microscopy (SEM) was performed, and the final coatings' images on the glass surface are shown in Figure 5. Initially, the glass surface appears to be smooth. A continuous coating with a few minor excrescences was seen with 0.3 weight percent of silica nanoparticles applied and a

Table 1 — Elemental weight % and atomic % of original Silica Nanoparticles

Element	Wt%	Atomic %
O	51.85	65.4
Si	48.15	34.6
Total:	100	100

Table 2 — Elemental weight % and atomic % of HDTMS-nano-SiO<sub>2</sub> Nanoparticles used for experimentation

Element	Wt %	Atomic %
C	19.9	29.18
O	43.49	47.86
Si	36.61	22.96
Total:	100	100

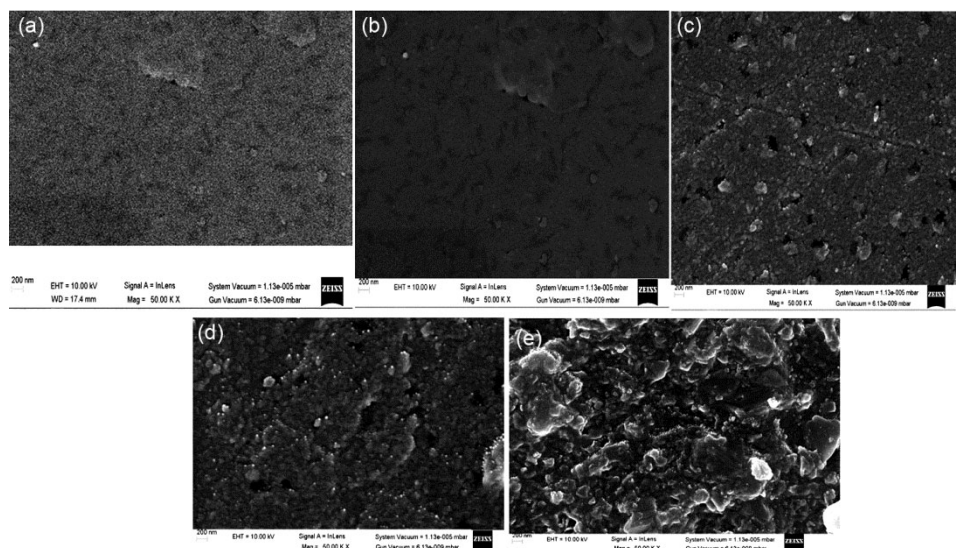


Fig. 5 — shows SEM of the original glass surface (a) and glass surface modified with varying silica nanoparticles concentrations (b) 0.3 wt%, (c) 0.6 wt%, (d) 2 wt%, & (e) 3.6-4 wt%, respectively having 50.00 K times magnification.

water contact angle of 144 degrees. Microscale isle-like structured agglomerations are formed when the concentration of silica nanoparticles increases to 0.6 weight percent. These aggregates have a high-water contact angle of 152 degrees because of their sufficient surface roughness. No sharp observable accession of the water contact angle had been seen until the concentration increased to 3.6 weight percent as per the specimen tested.

On the other hand, it is observed that when silica concentration increases, the coating thickness increases and becomes denser, possibly leading to cracks and other detrimental effects on the surfaces. This suggests that silica nanoparticle coatings are unsuitable for high silica concentrations. Therefore, a concentration of 0.25–1 weight percent is ideal in this instance, especially if superhydrophobicity and transparency are to be required simultaneously<sup>15</sup>.

When the concentration of silica nanoparticles is 0.6 weight percent or lesser, the coated glass exhibits a transmittance of more than 60%, which is distinctly comparable to bare glass. Surface roughness and film thickness both increase when the concentration exceeds 0.6 wt.%. As a result, transparency is decreased due to increased light scattering. Transparency and superhydrophobicity typically go hand in together<sup>16</sup>.

In contrast, it is possible that increased superhydrophobicity caused by surface roughness results in less transparency. To some extent, an increase in silica content can cause a decrease in

transparency and an increase in hydrophobicity. Hence, one of the most important elements in the creation of a superhydrophobic transparent surface is the correct concentration of silica. All things considered, the concentration up to 0.6 wt.% is appropriate in this instance for the discussed research work. Surface roughness and film thickness both increase when the concentration exceeds 0.6 wt.%. As a result, transparency is decreased due to increased light scattering. Superhydrophobicity and transparency generally contradict one another, and it is possible that increased superhydrophobicity caused by surface roughness results in decreased transparency. To a certain extent, an increase in silica content can cause a decrease in transparency and an increase in hydrophobicity. Hence, one of the most important elements in the creation of transparent superhydrophobic surfaces is the correct concentration. All things considered, the concentration of 0.6 wt.% is appropriate in this instance. It has been examined further that, surface coating with a concentration of up to 0.6 wt.% maintains its coating properties throughout the course of a month.

### 3.4 WCA Analysis

Water contact angle test (WCA) Analysis of the varying concentrations of silica nanoparticles viz. 0.3 wt%, 0.6 wt%, 2 wt%, and 3.6–4 wt% with respect to the original glass surface were performed and were respectively analyzed along with the nature of their hydrophobicity shown in Figure 6.

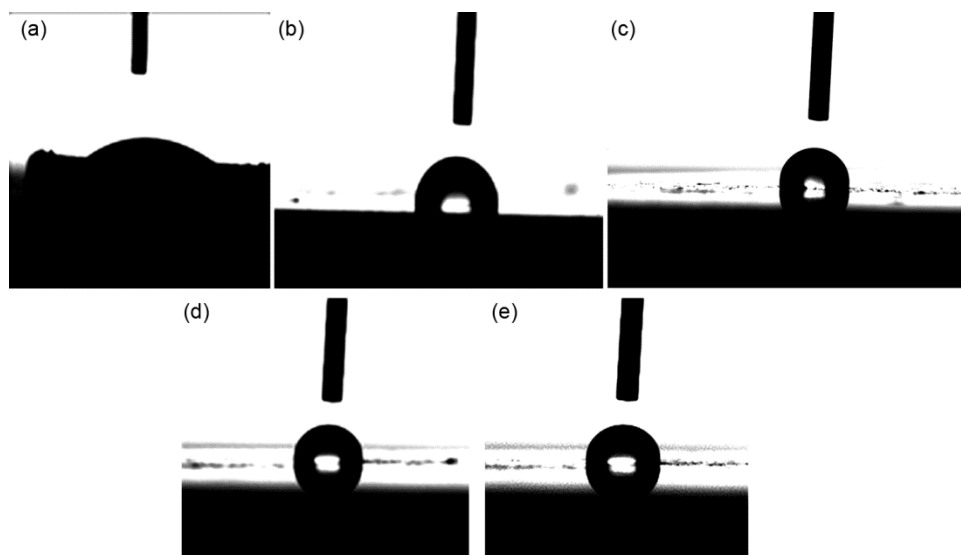


Fig. 6 — The WCA (water contact angle) of droplets of water on (a) the original glass surface, (b) HDTMS+0.3% Nano-SiO<sub>2</sub>, (c) HDTMS+0.6% Nano-SiO<sub>2</sub>, (d) HDTMS+2% Nano-SiO<sub>2</sub>, & (e) HDTMS+(3.6–4)% Nano-SiO<sub>2</sub>.

Table 3 — shows the WCA Analysis of the varying concentrations of silica nanoparticles along with the nature of their transparency

Sample	Type of Coating	Water Contact Angle (Degrees)	Nature of Hydrophobicity	Nature of Transparency
A	Original Glass Surface	52	Hydrophilic	Satisfactory
B	HDTMS+0.3%Nano-SiO <sub>2</sub>	144	Hydrophobic	Good
C	HDTMS+0.6%Nano-SiO <sub>2</sub>	152	Super Hydrophobic	Excellent
D	HDTMS+2.0%Nano-SiO <sub>2</sub>	155	Super Hydrophobic	Average
E	HDTMS+(3.6-4)%Nano-SiO <sub>2</sub>	155	Super Hydrophobic	Below Average

The transparency of the varying silica nanoparticles with HDTMS has been assessed demonstratively represented further by figure 9. The test results represent the HDTMS+0.6%Nano-SiO<sub>2</sub> being the most optimum concentration for achieving hydrophobicity and transparency at the same time.

Detailed information on the effect of varying the concentrations of the silica nanoparticles with that of the HDTMS on hydrophobicity and transparency has been summarized in Table 3.

The Cassie-Baxter and Wenzel models are typically used to explain the hydrophobic nature of the coatings with high roughness. Accordingly, as per the Wenzel model, water droplets adhere to a rough surface by following its profile, making it impossible for them to move over it<sup>17</sup>. Water droplets tend to slide across the surface of samples made of silica nanoparticles, demonstrating that our experimental results are better explained by the Cassie-Baxter hypothesis.

Therefore, the experimental outcome for WCA (water contact angle analysis) is concluded as follows:-

The smooth glass surface's water contact angle is found to be 52 degrees<sup>17</sup>. The fraction of air in contact with water droplets and the fraction of the solid surface in contact with water droplets are denoted by  $f_2$  and  $f_1$  respectively<sup>17</sup>; such that

$$f_2 + f_1 = 1 \quad \dots (1)$$

Also, Cassie's equation is mathematically represented as

$$\cos \theta_A = f_1 \cos \theta - f_2 \quad \dots (2)$$

In this equation, the apparent contact angle measured on the substrate surface is denoted by  $\theta_A$  and the  $\theta$  is the WCA (water contact angle) measured on the smooth surface which comes out to be 52° as already mentioned, which further indicates that the surface occupied by air is around 94.68%. With the help of the average water contact angle which is 152° the value of  $f_1$  calculated comes out to be 5.29%, which further represents that the combination of silica nanoparticles and HDTMS makes it simple for air to be trapped and generates a super-hydrophobic surface.

TGA GRAPH OF ORIGINAL NANOFILM (SILICA NANOPARTICLES)

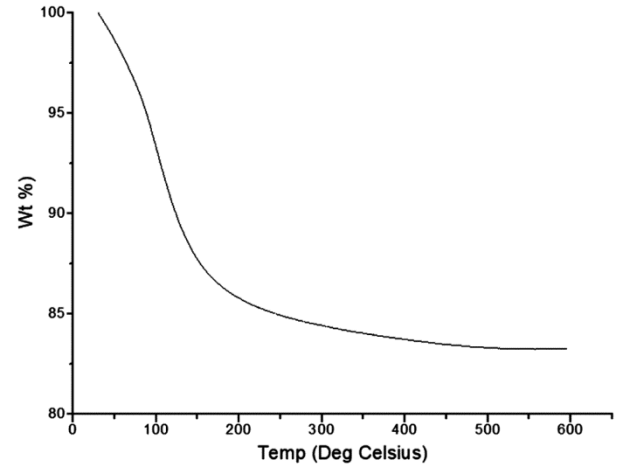


Fig. 7 — TGA Graph of the original Silica nanoparticles nanofilm

TGA GRAPH OF MODIFIED NANOFILM (SILICA NANOPARTICLES + HDTMS)

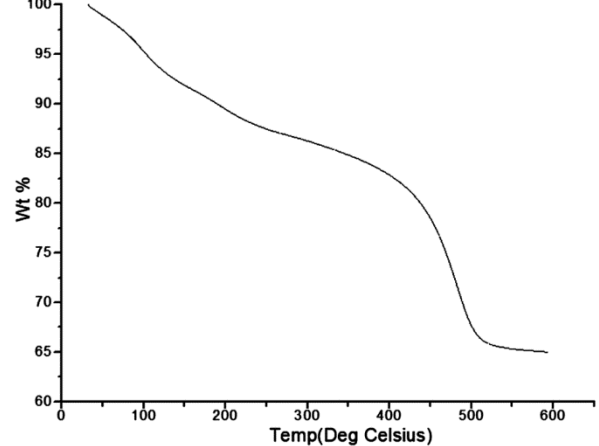


Fig. 8 — TGA Graph of the Modified Hydrophobic (0.6 % Silica nanoparticles + HDTMS) nanofilm.

As clearly evident in Table 3 the nano-coating with a water contact angle of 152 degrees demonstrates excellent superhydrophobicity and at the same time exhibits excellent transparency and environmental stability as discussed in detail later in Figures 9, 10, 11(a), and 11(b) respectively while being experimentally evaluated by coating the sample C on solar cells.

### 3.5 TGA Analysis

As shown in Figs 7 & 8, both nano-SiO<sub>2</sub> and HDTMS-nano-SiO<sub>2</sub> experienced a mass loss in the



20–150 °C range, with nano-SiO<sub>2</sub> experiencing a greater mass loss as compared to HDTMS-nano-SiO<sub>2</sub> observed by the thermogravimetric analysis (TGA).

On the nano-SiO<sub>2</sub> surface, hydroxyl(-OH-) groups were assumed to be the primary cause of mass loss when combined with TGA analysis. The mass loss of nano-SiO<sub>2</sub> with rising temperature was extremely modest, and the final mass stayed at around 90%.

However, the HDTMS-nano-SiO<sub>2</sub> underwent the second breakdown in the 400–500 °C temperature range, leading to a significant fall of the sample mass with only around 65% of the final mass.

This degradation was mostly brought by the long-chain alkyl disintegration on the sample's surface.

This demonstrated that CH<sub>2</sub>(CH<sub>2</sub>)<sub>14</sub>CH<sub>3</sub> could be effectively ingrafted onto the surface of HDTMS-nano-SiO<sub>2</sub>. Hence, results successfully infer that HDTMS-nano-SiO<sub>2</sub> is more stable at higher temperatures, particularly in the range of 20-150° Celsius compared to nano-SiO<sub>2</sub> and hence will remain stable at higher temperatures in outdoor environment conditions.

### 3.6 Demonstration of the assessment of the transparency of Nano coatings

For applications related to solar arrays, the coatings should be clear and not interfere with the glass's clarity and transparency. Further, the light should not be reflected or bent while traveling through the glass. The mentioned concept has been successfully demonstrated by checking the quality of transparency with the help of various glass slides with varying amounts of nanosilica. Figure 9 shows the outcomes of the experiment. Among all coatings, the addition of HDTMS increases transparency however its effectiveness is only when the nano-silica percentage is up to 0.6%. Increasing the concentration of nanosilica further reduces transparency. It proves that a specific amount of nano silica combined with HDTMS is required for surface transparency (experimentally validated through SEM results).

### 3.7 Assessment of the hydrophobicity, anti-dust properties, and outdoor stability of nano-layers

Dust particles can accumulate on the surface due to prevailing wind, road constructions, transport activities including automobiles, and industrial activities like mining, cement, etc. Most dust particles are assembled and concentrated on the hydrophilic surface where water drops present on the surface help to adhere a dust particle on the surface affecting transparency and power production, especially in the case of solar panels

making the condition worse in the case of the solar arrays. Hence, the coatings to be used for solar applications due to exposure to a harsh environment should exhibit a convincing anti-dust characteristic where a very low or absolutely no amount of dust is clearly observable on nanomaterial-coated surfaces as compared to uncoated surfaces.

In this work, of all the coatings described in relation to the optimum percentage of nano-silica which will give the perfect characteristic blend of optical transparency and hydrophobicity coating having 0.6% by wt. of nano-silica has been chosen and has been tested for environmental stability in relation to its anti-dust property and hydrophobicity and results show no dust accumulation whatsoever for the mentioned coatings.

It is well-known that a solar PV panel's total efficiency is directly related and proportionate to its output power<sup>18</sup>. As a result, the total efficiency increases as the output power increases.

Further, for the validation of the evaluation 40-day exhaustive experiment was carried out including a nano-material-coated solar cell, a solar cell that was cleaned every day, and a solar cell on which dust was intentionally allowed to settle down (as shown in Fig. 11(a)) without any cleaning procedure to understand the relation between the effect of nano-material coating on the solar cell and its output power. As a result, the penetration of photons was reduced,

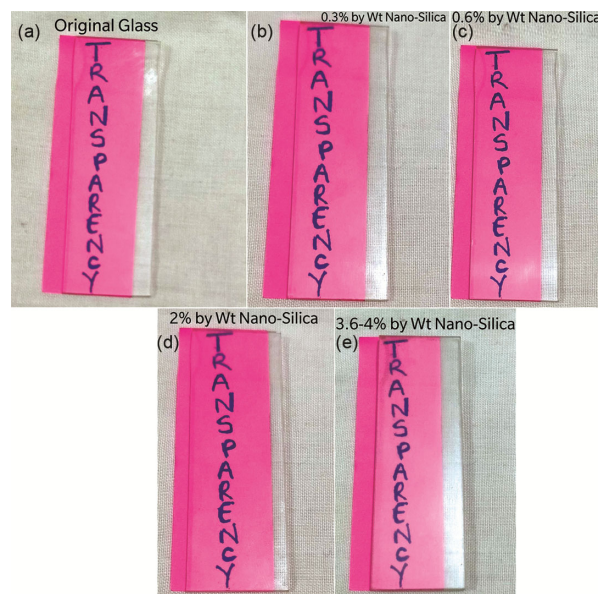


Fig. 9 — represents the Impact of Transparency after gradually increasing the concentration of nano silica a) Original glass b) 0.3% nano-silica concentration, c) 0.6% nano-silica concentration, d) 2% nano-silica concentration, & e) 3.6-4% nano-silica concentration.

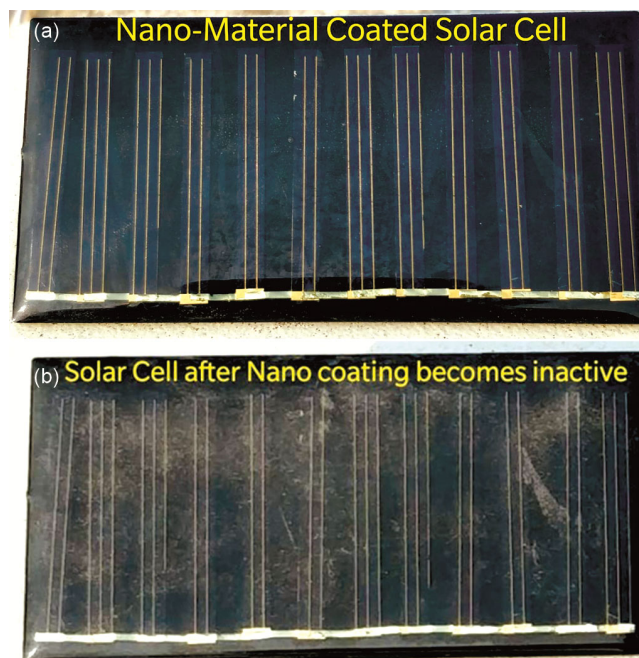


Fig. 10 — (a) Condition of the solar cell surface with nano-coating on the first day of environmental exposure with no sign of dust settlement on its surface, & (b) shows the condition of the solar cell surface with no nano-coating left on the surface because of the dust settlement on its surface after 40 days of experimentation.

lowering the overall efficiency of the solar PV cell further. When compared to the dusty solar cell, the uncoated solar cell that was physically cleaned boosted its output power by 10%.

Further in this concern, when the water drop is poured on the coated glass of the solar cell, it rolls down very fast courtesy of the hydrophobic characteristic achieved by the nano-silica modified to HDTMS-nano-silica confirmed by the WCA test of HDTMS-nano-silica. Due to this HDTMS-nano-silica coated surface collects the dust particles effectively whereas, in the case of uncoated glass, the water drop moves down slowly and without collecting dust particles. Further, it was investigated that the water droplets dropped over the nanomaterial-coated solar cell rolled down extremely quickly gathering dust particles with them leading to the efficient performance of solar cell in the dusty environment of the testing site which is validated by the fact that output power produced by the nanomaterial-coated solar cell is way greater than the average power rating of a solar cell given by the manufacturer which is around (200-210) mW.

Additionally, the physical cleaning of solar PV systems is tedious, expensive, and dangerous, and it may result in rusting of the frame of the panel. Using the transparent, hydrophobic self-cleaning HDTMS-

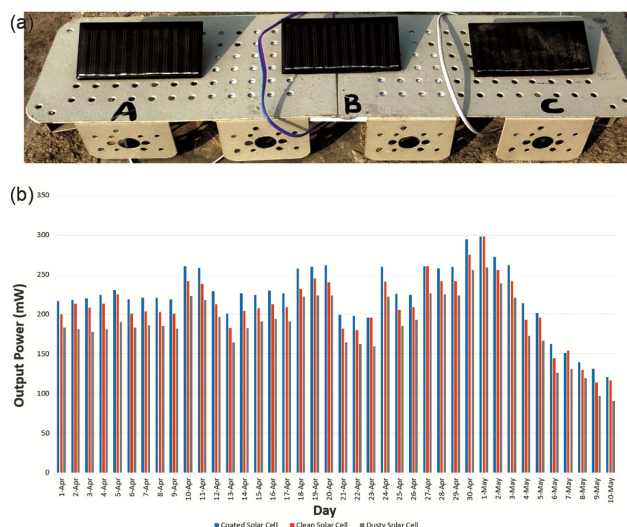


Fig. 11 — (a) shows the (A) nanocoated uncleaned solar cell, (B) physically cleaned uncoated solar cell, and (C) uncoated uncleaned dusty solar cell, & (b) shows the average power generated by them for 40 days installed at the site of experimentation during (April-May) 2022.

nano-SiO<sub>2</sub> coating, on the contrary, boosts the output power by 16% when compared to the dusty solar cell which is used as the reference and by 6.5% when compared to the uncoated manually cleaned solar cell, as represented in Figure 11.

The solar cell's maximum output power was measured with respect to the maximum solar radiation per day. Lastly, on assessing the results, it was found that out of 40 days of experimental investigation, the coating remained successfully active and stable for 35 days in the external environment as for 35 straight days the output of the nano-coated solar cell was well above the rated average power of the solar cell provided by the manufacturer. But after 35 days, the solar cell output starts decreasing, stating that mentioned nano-coatings can be successfully used for 35 days from their first application.

#### 4 Conclusion

Modified superhydrophobic HDTMS-nano-SiO<sub>2</sub> coatings with enhanced transparency and anti-dust properties for photovoltaic applications have been synthesized and characterized successfully and demonstrated experimentally. The synthesis technique of coatings using the single-step dip-coating approach discussed in this research work is very facile and intelligible. It does not require the substrate to be treated beforehand or afterward and hence can be fabricated in large quantities on a variety of substrates without any additional surface modification.



The nano-coating synthesized using the discussed technique has strong industrial feasibility and hence can be a strong and potential alternative to other conventional nano-coatings to a great extent. The enhanced properties of the nano-coatings lead to an increase in the output power of solar PV cells greater than the rated average power of the cells during the active period of the nano-coatings.

The most optimized nano coating has been found to be HDTMS+0.6% nano-SiO<sub>2</sub> because of its exceptional superhydrophobicity, transparency, good stability on surfaces at high temperatures up to 150°C with significantly low mass loss, and enhanced environmental stability and efficiency when tested after being applied on the surface of the solar cell. The nanocoatings have been found to be stable for up to 1 month and 5 days in an external environment and after that period the coating becomes inactive, which is observed by the reduction of the solar cell's output power below the solar cell's average rated power.

Thus, the nano-coatings mentioned in the research work can be prepared with cost-effective chemicals hence the nano-coatings produced by the discussed method prove to be extremely economical and pocket-friendly for the large-scale sector of solar arrays and solar farms by reducing the maintenance costs of cleaning to an impactful and significant level and hence can increase the overall efficiency of the solar array significantly and convincingly due to no soiling effects on solar panels for a considerable period.

### Acknowledgments

The authors hereby acknowledge IIT Ropar, IIT Roorkee, and CRS laboratory, Applied Physics, JEC, Jabalpur, M.P., India for using synthesis and characterization facilities.

### References

- Xu B & Zhang Q, *ACS Omega*, 6 (2021) 9764.
- Hsu C C, Lan W L, Chen N P & Wu C C, *Opt Laser Technol*, 58 (2014) 202.
- Song H Z & Zheng L W, *Cellulose*, 20 (2013) 1737.
- Huang Q B, Xu M M, Sun R C & Wang X H, *Ind Crops Prod*, 85 (2016) 198.
- Wu G M, Liu D, Chen J, Liu G F & Kong Z W, *Prog Org Coat*, 127 (2019) 80.
- Rukmanikrishnan B, Jo C H, Choi S J, Ramalingam S & Lee J, *ACS Omega*, 5 (2020) 28767.
- Xiong M M, Ren Z H & Liu W J, *J Dispersion Sci Technol*, 41 (2020) 1703.
- Li L, Li B, Dong J & Zhang J, *Journal of Materials Chemistry A*, 4 (2016) 13677.
- Latthe S, Terashima C, Nakata K & Fujishima A, *Molecules*, 19 (2014) 4256.
- Lee S G, Lim H S, Lee D Y, Kwak D & Cho K, *Adv Funct Mater*, 23 (2013) 547.
- Darband G H, Aliofkhaezrai, Khorsand S, Sokhanvar S & Kaboli A, *Arabian Journal of chemistry*, 13 (2020) 1763.
- Zhou H, Wang H, Niu H, Gestos A & Lin T, *Adv Funct Mater*, 23 (2013) 1664.
- Meena M K, Sinhamahapatra A & Kumar A, *Colloid Polym Sci*, 297 (2019) 1499.
- Zhang Q & Xu B, *ACS Omega*, 6 (2021) 9764.
- Parvate S, Dixit P & Chhatopadhyay S, *J. Phys. Chem. B*, 124 (2020) 1323.
- Wang C, Wu A & Lamb R, *J. Phys. Chem. C*, 118 (2014) 5328.
- Liu J, Janjua Z A, Roe M, Xu F, Turnbull B, Choi K S, Hou X, *Nanomaterials*, 6 (2016) 232.
- Hassan M K, Alqurashi I M, Salama A E, Mohamed A F, *J Umm Al-Qura Univ Eng Archit*, 13 (2022) 18.
- Zheng Xuwen, Xu Wenyuan & Xie Shuangrui, *Materials*, 14 (2021) 5672.
- Aljallis E, Sarshar M A, Datla R, Sikka V, Jones A & Choi C, *Phys Fluids*, 25 (2013) 025103.
- Lin Y F, Chen C H, Tung K L, Wei T Y, Lu S Y & Chang K S, *ChemSusChem*, 6 (2013) 437.
- Liu Jin-Qiu, Bai Chong, Jia De-Dong, Liu Wei-Liang, He Fu-Yan, Liu Fu-Yan, Yao Jin-Shui, Wang Xin-Qiang & Wu Yong-Zhong, *RSC Adv*, 4 (2014) 18025.
- Zhang Y, Fang F, Wang C, Wang L D, Wang X J, Chu X Y, Li J H, Fang X, Wei Z P, Wang X H, *Polym Compos*, 35 (2014) 1204.
- Paz C V, Vásquez S R, Flores N, García L & Rico JL, *Mater Res Express*, 5 (2018) 015314.
- Yu F & Huang H X, *Polym Test*, 45 (2015) 107.
- Yu Bing, Cong Hailin, Xue Lei, Tian Chao, Xu Xiaodan, Peng Qiaohong & Yang Shujing, *Anal Methods*, 8 (2016) 919.
- Cheng, D, Wen Y B, An X Y, Zhu X H & Ni Y H, *Carbohydrate Polymers*, 151 (2016) 326.
- Dou W W, Wang P, Zhang D & Yu J Q, *Materials Letters*, 167 (2016) 69.
- Petcu C, Purcar V, Spataru C I, Alexandrescu E, Somoghi R, Trica B, Nitu S G, Panaitescu D M, Donescu D & Jecu M L, *Nanomaterials*, 7 (2017) 47.
- Zhang H Y, Li B B, Sun D, Miao X L & Gu Y L, *Desalination*, 429 (2018) 33.
- Sohrabi B, Mansouri F & Khalifa S Z, *Progress in Organic Coatings*, 131 (2019) 73.
- Valluri, S. K., Schoenitz, M., & Dreizin, E. (2020), *Nanomaterials*, 10 (2020) 2367.
- Singh P & Saroj A L, *Polymer Plastics Technology and Materials*, 60 (2021) 298.